### IN HONOUR OF DES WALLING

WILEY

# Proglacial river sediment fluxes in the southeastern Tibetan Plateau: Mingyong Glacier in the Upper Mekong River

Xixi Lu<sup>1</sup> | Ting Zhang<sup>1</sup> | Boey Lai Hsia<sup>2</sup> | Dongfeng Li<sup>1</sup> | Heather Fair<sup>3,4,5</sup> | Hewen Niu<sup>6</sup> | Samuel D. X. Chua<sup>1</sup> | Li Li<sup>2</sup> | Shaojuan Li<sup>2</sup>

#### Correspondence

Xixi Lu and Ting Zhang, Department of Geography, National University of Singapore, 10 Kent Ridge Crescent, Singapore 119260, Singapore.

Email: geoluxx@nus.edu.sg and zhang\_ting@u.

### **Funding information**

Ministry of Education - Singapore; National University of Singapore, Grant/Award Number: A-0003626-00-00; Yunnan University of Finance and Economics

### **Abstract**

Glacial and proglacial erosion are important sediment sources in river basins. The retreat of many glaciers on the Tibetan Plateau has important implications on the supply of fresh water and sediment dynamics for downstream river basins. Despite the importance of water and sediment dynamics at these catchments, existing quantification of suspended sediment fluxes from glacial catchments on the Tibetan Plateau is limited due to poor accessibility and challenging environments. This study presents the results of in-situ investigations of water discharge and suspended sediment fluxes from the Mingyong Glacier catchment in Yunnan, Southwest China, between August 2013 and July 2017. The results show that the variation in water discharge and suspended sediment was highly seasonal. The variation of average suspended sediment concentration was large-69  $\pm$  45; 119  $\pm$  104; and 94  $\pm$  97 mg/L in 2013, 2015, and 2016, respectively. We estimate that the sediment yield from the Mingyong catchment was highly variable ranging from 1104 t/km<sup>2</sup>/year in 2013 to 2281 t/km<sup>2</sup>/year in 2016, with 65%–78% of the total annual sediment load occurring during the summer (June to August). These annual variations in sediment yield can be attributed largely to precipitation patterns and extreme melting events. This study has provided a benchmark dataset that can be used for further works that investigate the impact of climate change on sediment dynamics in glacierized catchments in the Tibetan Plateau. Subsequently, the study helps us to better understand the increasing sediment supply to the Upper Mekong River from glacierized headwater catchments.

### KEYWORDS

China, Mekong River, proglacial river, sediment fluxes, water discharge, Yunnan

### 1 | INTRODUCTION

The meltwater from glaciers on the Tibetan Plateau feeds many large Asian rivers, for example, the Indus, Ganges, Brahmaputra, Salween, Mekong, Tarim, and Syr Darya Rivers (Li, Lu, et al., 2021; Li, Overeem, et al., 2021). Millions of people in the region depend on the rivers for their livelihoods. With an average elevation exceeding 3000 m a.s.l., the Tibetan Plateau contains around 36 800 glaciers occupying a total area of ~50 000 km² (Yao et al., 2012). The physical geographic

conditions of the Tibetan Plateau amplify its susceptibility to solar radiation and sensitivity to global warming (Pepin et al., 2015). Yao et al. (2012) reported that glacial retreat on the Tibetan Plateau has intensified since the 1990s.

Glaciers are powerful agents of erosion through denudation mechanisms, generating large amounts of glacial debris in the process. Thus, sediment yields from glacial basins are higher than the global average (Hallet et al., 1996). Suspended sediment fluxes from proglacial areas, accompanied by intensified meltwater and increased

<sup>&</sup>lt;sup>1</sup>Department of Geography, National University of Singapore, Singapore, Singapore

<sup>&</sup>lt;sup>2</sup>School of Urban Management and Resource Environment, Yunnan University of Finance and Economics, Kunming, China

<sup>&</sup>lt;sup>3</sup>National Science Foundation Postdoctoral Research Fellow in Biology, University of Minnesota, Minneapolis, Minnesota, USA

<sup>&</sup>lt;sup>4</sup>Institute of Mountain Hazards and Environment, Chinese Academy of Sciences, Chengdu, China

<sup>&</sup>lt;sup>5</sup>USDA Agricultural Research Service, Columbus, Ohio, USA

<sup>&</sup>lt;sup>6</sup>State Key Laboratory of Cryospheric Sciences, Northwest Institute of Eco-Environment and Resources, Chinese Academy of Sciences. Lanzhou. China

sediment availability, have increased in response to accelerated glacier retreat (Li, Lu, et al., 2021; Li, Overeem, et al., 2021; Overeem et al., 2017). In glacier regions, the roles of sediment are double-edged—while it is essential in the maintenance of riverine ecology, morphology, agriculture, and fisheries by providing nutrients and materials (Walling, 2006), sediments also adsorb toxic chemicals such as mercury. Therefore, high concentrations of sediment degrade water quality, alter aquatic habitats, and cause civil engineering problems for dams and river transportation (Li, Lu, et al., 2021; Li, Overeem, et al., 2021). Furthermore, given the context of climate change, understanding sediment dynamics from glacial catchments originating on the Tibetan Plateau is important for downstream land resource management and planning (Li, Lu, et al., 2021; Li, Overeem, et al., 2021).

Sediment transport varies spatially along proglacial rivers and is characterized by strong seasonal and diurnal variabilities (Beylich et al., 2017). Proglacial sediment is predominantly produced by glacial movement and is transported by glacial meltwater originating from the melting of ice on the ice surface (supraglacial), at the bed (subglacial), and within the glacier (englacial) (Heckmann et al., 2016). Heat required to melt the ice can be supplied by solar radiation or geothermal heat beneath the glacier (Bennett & Glasser, 2011). Therefore, proglacial discharge hydrographs follow the temporal changes in solar incidence on annual and diurnal timescales (Miles et al., 2020). Moreover, the rates at which meltwater and sediment are drained depend on the type of glacial meltwater pathways and the stream channel size (Carrivick & Tweed, 2021).

Previous studies on the quantification of suspended sediment load on the Tibetan Plateau are mostly derived from hydrological gauging stations that are located far away from the glaciers (Li, Lu, et al., 2021; Li, Overeem, et al., 2021; Shi et al., 2018). In addition, field measurements of suspended sediment fluxes from proglacial rivers on the Tibetan Plateau are very limited and spatially scattered. For example, Kumar et al. (2002) measured discharge and suspended sediment in the meltwater of Gangotri Glacier in Garhwal Himalaya, India; Kumar et al. (2002) analysed the spatio-temporal trends of suspended sediment flux along the Sutlej River and its main tributaries in western Himalaya; and Srivastava et al. (2014) measured discharge and suspended sediment load in Dunagiri Glacier basin located in Garhwal Himalaya between 1984 and 1989. Nearer to Southeast Asia, studies that examined sediment loads in the Mekong basin have reported a lack of sediment data from the Upper Mekong located within China (Lu & Siew, 2006; Walling, 2008; Wang et al., 2011). Particularly, glaciated catchments are poorly studied, and to our best knowledge, there has been no study conducted that has quantified the sediment load in the Upper Mekong catchment within China.

Consequently, this study focuses on the Mingyong Glacier in Yunnan Province, which is located in the southeast region of the Tibetan Plateau. The glacier retreated by 190 m between 1998 and 2004, with 110 m of the retreat occurring between 2002 and 2004 (Baker & Moseley, 2007). Considering this reduction in glacier ice, knowledge about sediment delivery from the glacial catchments in the Upper Mekong basin is ever more important in the understanding of sediment delivery dynamics for the whole Mekong basin (Lu et al., 2014). Therefore, this study aims to: (1) quantify the sediment yield and

sediment load from the Mingyong glacial catchment; (2) analyse the temporal variability of suspended sediment flux from the Mingyong Glacier catchment; and (3) discuss the potential drivers and implications of changing sediment yield for the Upper Mekong basin in the context of climate change.

#### 2 | STUDY AREA

The Mingyong Glacier is a monsoonal temperate valley glacier situated in Deqin County, Yunnan Province in Southwest China (Figure 1). This glacial catchment was selected due to its position at the southeastern edge of the Tibetan Plateau, and as one of the lowest latitude glaciers in China, which renders it particularly sensitive to climate change (He et al., 2003; Liu et al., 2015). Being a part of the Three Parallel Rivers of Yunnan—the upper reaches of Yangtze, Mekong, and Salween—this area has received much attention from environmental conservationists due to its rich biodiversity and diverse ecosystems. The Mingyong Glacier flows from the east face of the Meili Snow Mountain Range into the Upper Mekong River (i.e., Lancang River). Thereafter, the Mekong continues its journey into the riparian countries of Myanmar, Laos, Thailand, Cambodia, and Vietnam. The total length of the Mekong River is 4350 km with a total drainage area of 795 000 km<sup>2</sup>.

The study site has a catchment area of 39.7 km² with 68% of the area covered by glaciers (27 km²). The elevation of the watershed ranges from 6684 m a.s.l at the Kawargarbo Peak to 2930 m a.s.l. at the glacier terminus with an average slope of 29% (Figure S1). The Mingyong Glacier icefall and tongue are covered by a layer of supraglacial debris that is contributed by sediments from the steep valley sides (Figure 2b). From the glacial terminus to the confluence with the Upper Mekong River, the Mingyong River flows for about 6.1 km. Due to accessibility issues, water samples and discharge measurements were taken from a single sampling station 3.1 km from the glacial terminus at an elevation of 2342 m a.s.l. (Figure S1). Specifically, the sampling station is located at 28°28′5.80″ N, 98°46′58.57″ E.

The Mingyong catchment is classified as a monsoon-influenced temperate oceanic climate—dry winters and warm, wet summers—under the Köppen-Geiger climate classification (Beck et al., 2018). At least 70% of its average annual precipitation is received during the warmest months (Figure 2c,d). Due to the lack of a weather station at Mingyong, annual climate data were taken from the nearest weather station 13 km away at Deqin. The average annual temperature in the catchment is  $5.6^{\circ}$ C and the average annual precipitation is 641 mm. Precipitation ranges from 6 mm in December to 133 mm in July. The average temperature is lowest at  $-2.2^{\circ}$ C in January and greatest at  $12.7^{\circ}$ C in July.

### 3 | METHODS

### 3.1 | Measurement of discharge

The Mingyong Glacier river does not have a stream gauging station; hence the discharge was manually measured and calculated (Figure S2). Flow velocity and water depth were measured during

1002/hyp.14751 by UNIVERSITY OF MINNESOTA 170 WILSON LIBRARY, Wiley Online Library on [21/11/2022]. See the

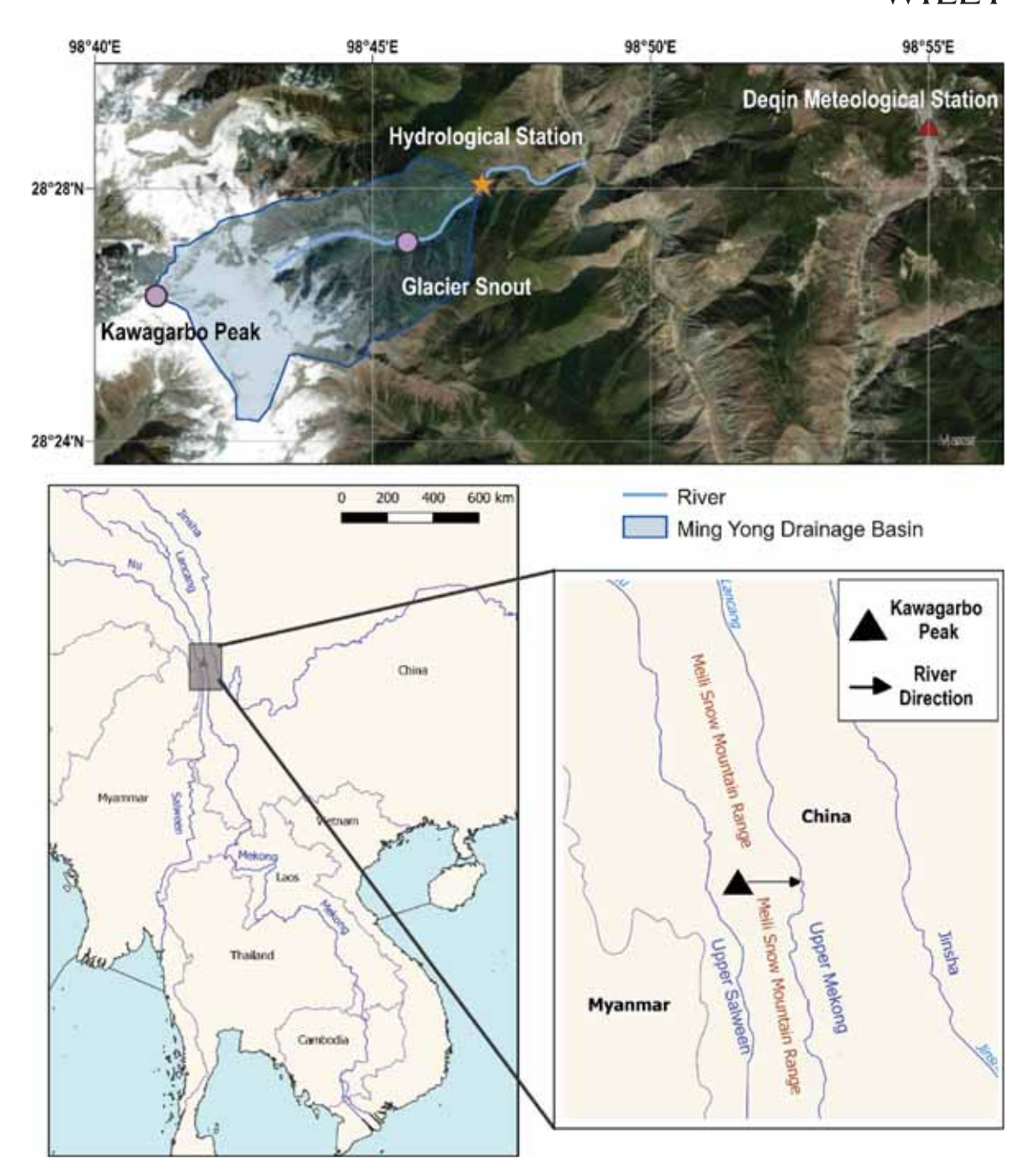


FIGURE 1 Location map of the study area. Mingyong glacial catchment from Google Earth (top), the Three Parallel River region (the Upper Yangtze, the Upper Mekong, and the Upper Salween) (bottom left), and the Meili Snow Mountain between the Upper Mekong River (Lancang River) and the Upper Salween River (Nu River)

each sampling event using the float method and meter rule (Figure S2), respectively. The cross-sectional area of the channel was measured in February 2014, September 2015, November 2016, and April 2017 (Figure S2c) because of danger when conducting measurements during the high-flow summer discharge. To calculate the cross-sectional area, the width of the river channel under bankfull conditions was first measured using a tape measure. The width was divided into 20 equal transects and the height of the tape measure to the riverbed was measured at each transect. The cross-sectional area was thus obtained by the sum of all transects (height × width of transect). Discharge was then calculated using the following formula:

$$Q = A \times V$$
,

where, Q is water discharge (m<sup>3</sup>/s), A is the cross-sectional area of the river channel (m<sup>2</sup>), and V is the flow velocity (m/s).

### 3.2 | Water samples collection

Because a significant proportion of suspended sediment is transported during infrequent high flows (Mao et al., 2019) from June to August, the frequency of collection was higher during periods of high

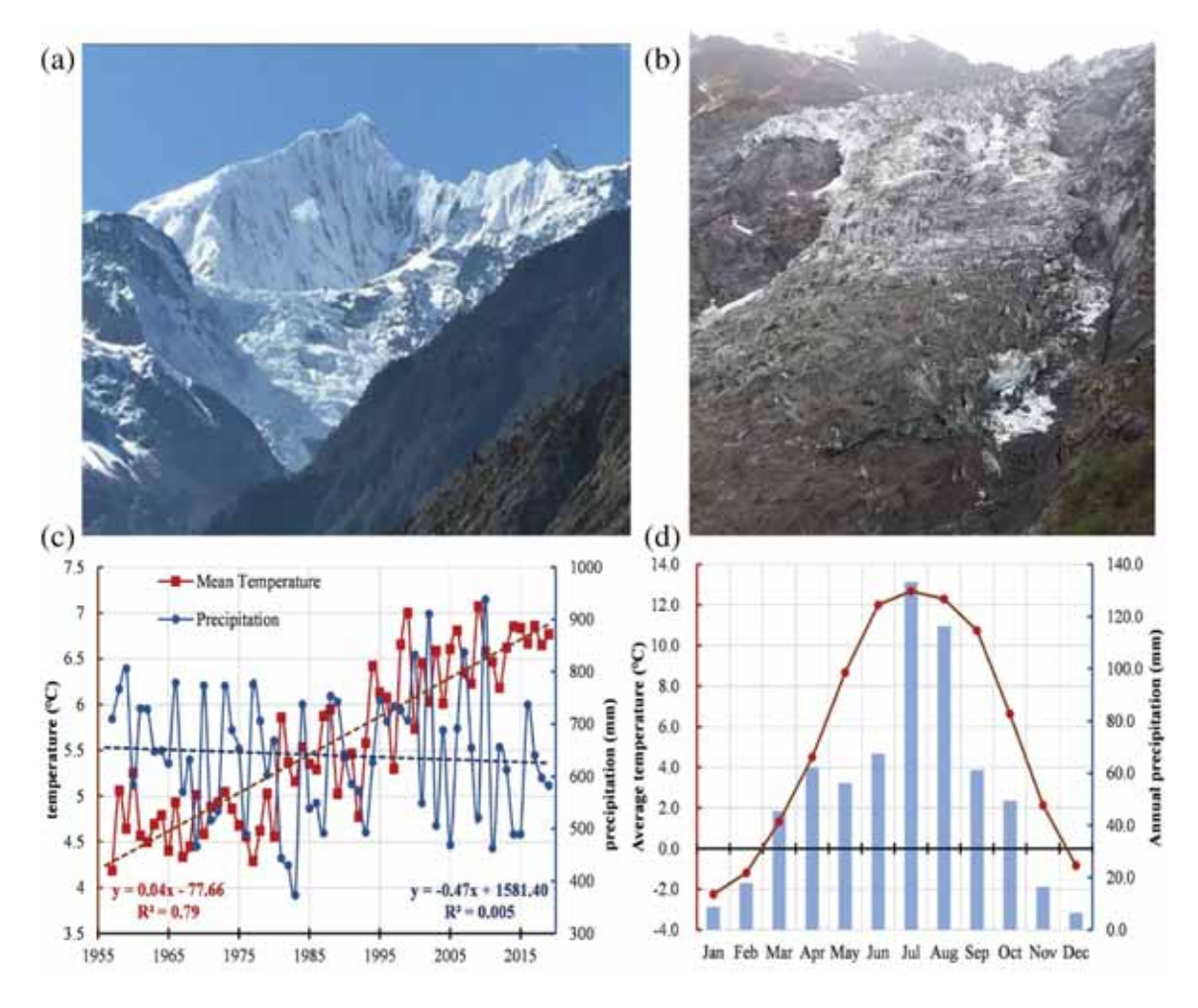


**FIGURE 2** Geomorphic and climatic characteristics of the Mingyong Glacier catchment. (a) Field photo of Kawagarbo Peak, and (b) field photo of Mingyong glacier icefall covered with supraglacial debris (photo credit: Boey Lai Hsia, 2013). (c) Long term changes in temperature and precipitation and (d) monthly variations in temperature and precipitation near the study site at Degin, 3000 m a.s.l

flow to capture the high transport rates. Following the average monthly precipitation and temperature (Figure 2d), five to six samples were collected during periods of high flows from June to August, and at least two samples were collected during periods of low flows from October to March (see Table S1 for the sampling frequency for each month). In total there were 158 sampling events from August 2013 to July 2017 with a gap from September 2014 to August 2015 due to manpower and logistical constraints.

# 3.3 | Measurement of suspended sediment concentration (SSC)

Except near the riverbed, mixing of suspended sediments streams is fairly homogenous throughout the cross-section because of turbulent flow. Thus, collection of water samples was done at a turbulent section to allow vertical and horizontal mixing of sediments. The sampling bottles were fully submerged and capped when fully filled. Three 500 ml water samples were collected per sampling event. Each bottle of water sample was filtered using 0.45  $\mu$ m pore size, 47 mm-

diameter Whatman nylon membrane filters and a Nalgene vacuum pump and filtration unit. The filter papers were air-dried for 3 days in the field to remove moisture before being individually stored in aluminium foil and resealable plastic bags. Suspended sediment mass was obtained in the laboratory by weighing the dried samples. The average mass of suspended sediment per sampling event (mg/500 ml) was multiplied by two to obtain the average SSC in mg/L.

Another characteristic of suspended sediment concentration during high flow is the increased variability of sediment concentration. Therefore, more sampling should take place during periods of high discharge. Storms make access difficult and measurements hazardous. Nevertheless, high-resolution data collected during high flows are essential for the development of good sediment rating curves. Due to the infrequency of high flows and logistical problems, collecting adequate high flow measurements cannot be achieved through hand sampling alone.

Bedload could be very high for the turbulent glacial stream, as indicated by the large size of boulders and bed materials, and irregular shape of the channel bed (Figure S2). Attempts were made to collect

the bedload materials and quantify the bedload. However, due to the lack of facilities and experienced personnel we were unable to conduct a sufficient number of bedload measurements.

### 3.4 | Sediment rating curves

Strong correlation is often observed between suspended sediment concentration and discharge in most streams. Compared to large river systems that usually contain an abundance of materials, the suspended load of small mountain streams usually depends on episodic events that transport fine materials from banks and upland areas Thus, suspended sediment concentration depends on both supply of sediments and discharge (Yaksich & Verhoff, 1983; Zhang et al., 2021). Nonetheless, suspended sediment concentration and discharge can be plotted to create what is known as a sediment rating curve. One benefit of developing a sediment rating curve is that it can be applied to interpolate missing data during the observation period (Asselman, 2000). We used a power function to fit the sediment rating curve expressed as:

$$SSC = a \times Q^b$$
,

where, SSC is in mg/L, Q is the water discharge (in m<sup>3</sup>/s), and a and b are fitting coefficients.

When b > 1, the increase in sediment volume per one unit of flow volume could result in a nonlinear relationship. Such situations imply that more than half of the sediment load is carried by high flows that account for less than 15% of the water volume or less than 5% of the period of measurement.

Suspended sediment rating curves were determined for Mingyong glacial catchment using discharge and suspended sediment concentration data between August 2013 and July 2017. The rating curves were fit by nonlinear least-squares curve fitting using the Levenberg-Marquardt (L-M) algorithm produced in Origin 2021b. One of the major limitations of the sediment rating curve is the assumption that the rating coefficients will remain constant (Zhang et al., 2021). As mentioned by Yaksich and Verhoff (1983), small mountainous catchments are often classified as 'event response' streams, which causes large scatter between sediment concentration and discharge and hence poorer relationships between suspended sediment concentration and discharge. The low accuracy of the sediment rating curves may be attributed partly to hysteretic effects, where at a given discharge, the sediment concentration on the rising and falling stage of the hydrograph differs (Khanchoul & Jansson, 2008). Separate rating curves are needed for the rising and falling limbs to account for seasonal variations so as to enhance the accuracy of the estimated suspended sediment concentration (Khanchoul & Jansson, 2008). In this study, the hydrological year is defined as August to July, with the rising stage occurring from February through July and the falling stage occurring from August through January.

# 3.5 | Estimation of sediment fluxes and sediment yields

Water discharge values were interpolated using a linear equation between the two closest sampling dates to obtain the daily sediment load for days without measurements. Due to interannual variation in SSC dynamics, rating curves derived using data from the falling and rising stages of the respective hydrological years were used to calculate the daily sediment load. The sediment load (SL; tons/day) was calculated using the following formula:

$$SL = Q \times SSC$$
,

where, Q is the water discharge  $(m^3/s)$  and SSC is the suspended sediment concentration (mg/L). The monthly sediment load was derived by summing estimated daily sediment loads for the respective month.

Sediment yield is defined as the amount of sediment per unit area removed from a watershed for a specific period of time. The sediment yield of a drainage basin, measured in tonnes/km² per annum, is the resultant effects of erosion, transportation and deposition occurring in the basin, and reflects the sediment delivery ratio within. Here, the sediment yield was calculated by dividing the annual sediment load by the size of Mingyong catchment area.

### 4 | RESULTS

# 4.1 | Suspended sediment concentrations and sediment rating curves

During the study period from August 2013 to July 2017 (Figure 3), the maximum discharge was  $36.1~\text{m}^3/\text{s}$  recorded on 1 August 2014, while the minimum discharge was  $2.1~\text{m}^3/\text{s}$  on 10 January 2017. The highest SSC (547.73~mg/L) was recorded on 1 August 2016, and the lowest SSC (0.2~mg/L) was recorded on 24 January 2017. Discharge-weighted mean SSC across the entire study period was 129.4 mg/L. Based on the hydrograph, the rising limb was between February and July and the falling limb was from August to January. The discharge and suspended sediment data were characterized by distinct seasonal variations (Figure 3). February accounted for the lowest monthly average discharge of  $3.89~\text{m}^3/\text{s}$  and January had the lowest monthly average SSC of 17.7 mg/L. Discharge increased in March and reached the peak in July, with the average discharge in July of  $31.85~\text{m}^3/\text{s}$  and the highest average SSC of 261.8~mg/L.

The  $R^2$  value for the SSC-Q rating curve for the entire study period was relatively low at 0.40 (p < 0.05; Figure 4a). The SSC-Q relation exhibited a large scatter for SSC for discharge values above 25 m³/s. Due to the poor fit, the rating curve was fitted by hydrological years to analyse the differences between each hydrological year (Figure 4b-d). The empirical relationship between SSC and discharge improved when the data was divided by hydrological years

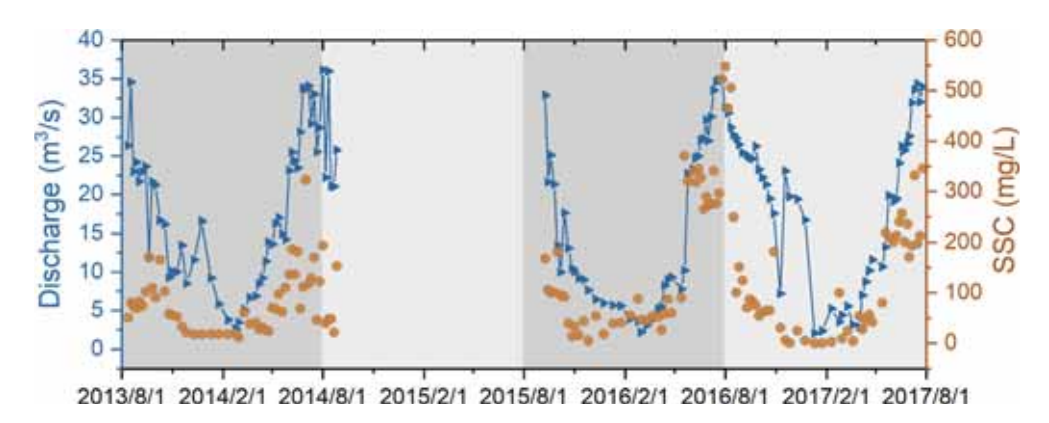
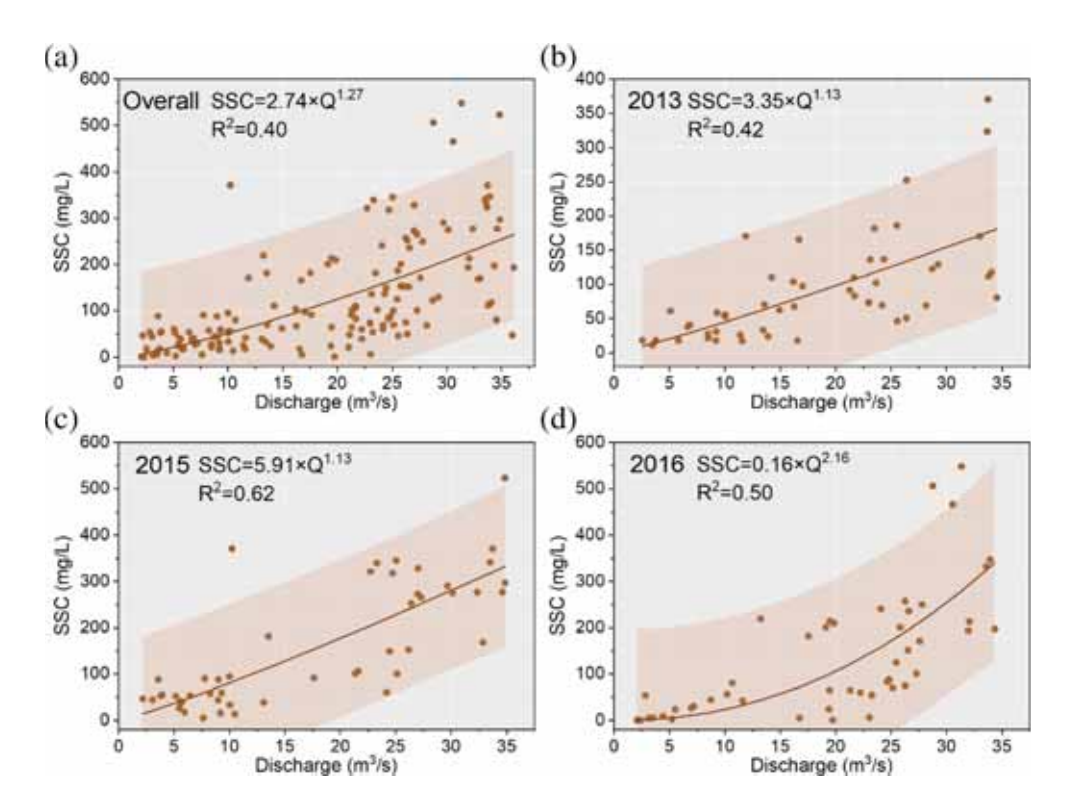


FIGURE 3 Observations of discharge and suspended sediment concentration (SSC) during three hydrological years. Observations of discharge are represented by blue triangles and observations of SSC are represented by orange dots



sediment concentration (SSC)–discharge (Q) rating curves, during (a) August 2013 to July 2017; (b) August 2013 to July 2014; (c) August 2015 to July 2016; (d) August 2016 to July 2017. The brown lines represent the sediment rating curves fitted by the corresponding SSC-Q scatter. The shaded area indicates a 95% confidence interval

 TABLE 1
 Sediment rating curves during the falling and rising stages at Mingyong River

Year	Sediment rating curve in the falling stage (August–January)	$R^2$	Sediment rating curve in the rising stage (February–July)	R <sup>2</sup>
2013	$SSC = 5.2474 \times Q^{0.8612}$	0.11	$SSC = 4.9034 \times Q^{0.9942}$	0.54
2015	$SSC = 2.0104 \times Q^{1.3156}$	0.67	$SSC = 15.6770 \times Q^{0.8858}$	0.74
2016	$SSC = 0.0360 \times Q^{2.4087}$	0.57	$SSC = 1.4774 \times Q^{1.5286}$	0.75

(Figure 4b–d). In particular, the largest  $R^2$  value can be found in the hydrological year of 2015 ( $R^2=0.62$ ). Scatter plots for 2015 and 2016 showed distinct power-law increases in SSC for discharge above  $20~\text{m}^3/\text{s}$ .

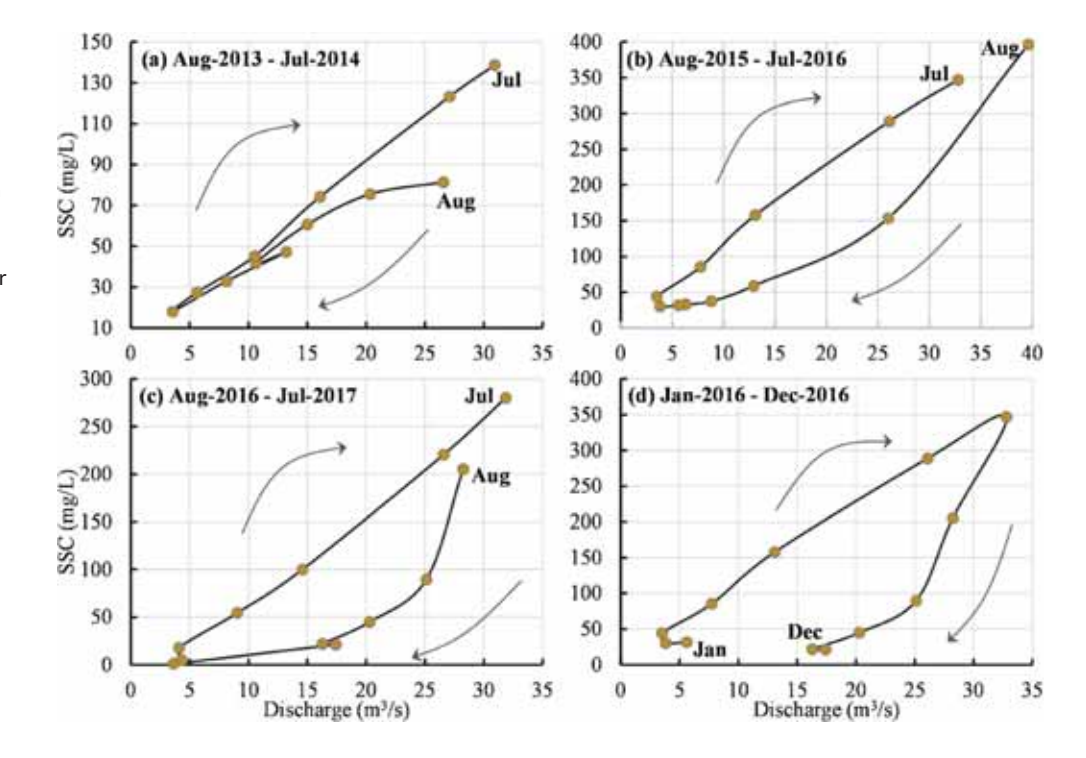
For discharge above 25 m<sup>3</sup>/s (Figure 4b–d), which were recorded during ablation seasons, large scatters were observed for all three hydrological years The data was further analysed by considering its inter-annual seasonal variations (Figure S3 and Table 1). Subsequently, the SSC-Q relationship improved when the data was categorized into falling and rising stages throughout the study period. However, during

the falling stage from August 2013 to January 2014, there was still no significant correlation between discharge and SSC ( $R^2=0.11$ ). The coefficient of correlation was higher during the rising stage than the falling stage for all hydrological years.

## 4.2 | SSC-Q hysteresis

Temporal analyses on discharge and suspended sediment concentrations were conducted to understand the behaviour of the suspended

sediment concentration (SSC)–discharge hysteresis loops for Mingyong catchment across three hydrological years and one calendar year. (a–c) Hysteresis in the hydrological year of 2013, 2015, and 2016, respectively; (d) hysteresis in the calendar year of 2016. The starting month and ending month are marked for each hysteresis loop



sediment hysteresis loops. In this study, hysteresis loops were plotted based on the average monthly *Q* values against SSC values to obtain the variability patterns (Figure 5). Hysteresis loops for the three hydrological years were represented by clockwise hysteresis (Figure 5a-c), with a higher SSC-value on the rising limb than that for the same discharge on the falling limb. For instance, at the discharge of 25 m<sup>3</sup>/s, SSC was higher during the rising stage when compared to the falling stage (110 vs. 80 mg/L in 2013, 288 vs. 153 mg/L in 2015, and 220 vs. 90 mg/L in 2016). The patterns across the three hydrological years suggest the sediment availability is depleted by the end of the ablation season (the beginning of the falling limb), resulting in clockwise hysteresis loops. For clarity, the clockwise hysteresis loop for the entire 2016 is shown in Figure 5d.

Hysteresis loops provide information on the influence of different sources of runoff on suspended sediment transport within proglacial rivers (Williams, 1989), by depicting the relationship between the transport capacity of the river and its sediment supply (Zhang et al., 2021). For example, sediment that is stored during periods of low discharge and transported when discharge increases results in the SSC-Q pattern in the form of a loop rather than a straight line (Smith & Dragovich, 2009). The higher SSC during the rising limb of the hydrograph compared to the falling limb may be explained by proximal sediment sources during the rising limb, but insufficient sediment supply during the falling limb (Smith & Dragovich, 2009; Williams, 1989). For the Mingyong Glacier basin, the sediment is sourced from large amounts of debris generated by the glacial environment that are readily available for transport (Figure 2). However, during the falling stage, the suspended sediment concentrations tend to be lower due to the unavailability of sediment sources and the increase in base flow discharge from subsurface soils.

# 4.3 | Temporal variations of water discharge and sediment yields

Both water discharge and suspended sediment flux in the Mingyong catchment are characterized by seasonal variations (Figure 6). The monthly maximum sediment loads, all occurring in July, amounted to 12.5 kt (2014), 30.3 kt (2016), and 25.1 kt (2017). Of the total annual sediment load, the majority (65% in 2013, 73% in 2015, and 78% in 2016) was highly concentrated in the summer from June to August. In contrast, the dry season month of February had the lowest monthly load at around 0.25% of the total annual load. Concurrently, the monthly sediment load was significantly correlated with the monthly water discharge, with an  $R^2$  value of 0.82.

The water discharge for hydrological years 2013, 2015, and 2016 were as follows – 0.50, 0.46, and 0.53 km $^3$ /year, respectively. The discharge did not vary significantly, implying that during these 3 years there was little variation in annual water discharge for the Mingyong catchment. However, annual sediment load variability was large, ranging from 44 kilotons (kt) in 2013 to 91 kt in 2015, and 73 kt in 2016 (Figure 7). Together, the sediment yield for Mingyong glacial catchment was derived to be 1104 t/km $^2$ /year in 2013, 2281 t/km $^2$ /year in 2015, and 1833 t/km $^2$ /year in 2016.

### 5 | DISCUSSION

# 5.1 | Dominant control of sediment fluxes: temperature or precipitation?

The seasonal variations in discharge and sediment load are jointly controlled by air temperature and summer rainfall (Figure 7). At the

FIGURE 6 Monthly precipitation (P), temperature (T), water discharge (WD), sediment load (SL), and suspended sediment concentration (SSC) in the Mingyong Glacier catchment. (a) Shows the monthly values while (b) shows the cumulative monthly values.

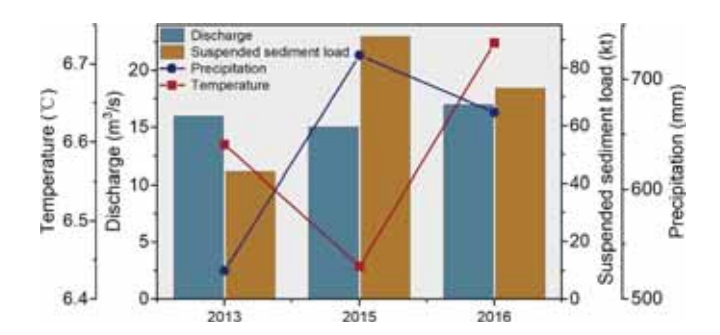


**FIGURE 7** Annual sediment load (brown bars), water discharge (grey-blue bars), precipitation (blue line), and temperature (red line) in the Mingyong Glacier catchment across the three hydrological years

Mingyong Glacier, fractures in the ice form crevasses, providing pathways for surface water to penetrate the glacier (Miles et al., 2020). In the summer, elevated air temperatures increase the surface melting and generate snow-glacier meltwater (Lau et al., 2010). The meltwater can flow from the surface of the glacier to the base through glacier conduits (Eyles, 2006), leading to higher meltwater flow velocity and capacity. As a result, there is an increase in meltwater erosion and sediment export (Delaney & Adhikari, 2020; Mao & Carrillo, 2017). Concurrently, the intense rainfall in July from the Indian monsoon increases the rate of exposed slope erosion and can trigger landslides and rock avalanches, leading to the observed high sediment loads

(Table S1) (Kirschbaum et al., 2020; Rosser, 2010). In other words, the discharge and suspended sediment load peaks observed in July can be explained by higher sediment accessibility, mobilization, and transport from the monsoon rainfall. Conversely, in the winter, reduced snow/glacier melting and the decreased rainfall causes the deformation of the glacial conduits. Furthermore, accumulated snow shields the underlying crevasses (Carrillo & Mao, 2020; Gatesman, 2017), thereby weakening erosion and reducing the transport of sediments into the proglacial stream (Table S1). The high sediment load during periods of high discharge suggests the predominance of supraglacial and subglacial sediment mobilization. However, more studies are needed to differentiate the transport of sediment load by meltwater or by precipitation.

Our observations show that there are large interannual variations of suspended sediment flux among the three hydrological years (2013, 2015, and 2016). The highest sediment yield occurred in 2015 (2283 t/km²/year), which is more than double the sediment yield in 2013 (1104 t/km²/year). These interannual variations seem to be mainly driven by the differences in annual precipitation rather than the mean annual temperature (Figure 6). Specifically, the highest annual precipitation was recorded in 2015, accompanied by a doubling of the number of extreme precipitation days (defined as daily precipitation over 20 mm) at the Deqin meteorological station. During a wetter hydrological year, the overall increased rainfall can increase the sediment transport capacity and evacuate more deposited

sediments from supra/sub-glacial debris and glacier valleys, causing a higher annual sediment yield (Delaney et al., 2018; Li et al., 2020; Micheletti & Lane, 2016). Concurrently, more frequent rainstorms enhance stream power and erosivity, thus increasing river channel erosion that can remobilize deposited sediments (Li, Lu, et al., 2021; Li, Overeem, et al., 2021; Lugon & Stoffel, 2010; Wulf et al., 2010). These extreme sediment events contribute disproportionally to the annual sediment yield and amplify the temporal variability in sediment transport (Lloyd et al., 2016; Wulf et al., 2012).

Simultaneously, temperature-sensitive glacier dynamics may also affect interannual variability in sediment yield (Costa et al., 2018; Stott & Mount, 2007). For example, the rate of glacier bedrock erosion or subglacial/proglacial sediment transport can be enhanced by the increased glacier melt flow due to higher temperatures (Chakrapani & Saini, 2009; Herman et al., 2021; Singh et al., 2020; Stott & Mount, 2007). However, the temperature variations detected within our study period pales in comparison to precipitation variations. Therefore, in the absence of extreme melting events that could shadow the impact of precipitation, we argue that the interannual variations in the sediment yield in the Mingyong Glacier catchment are largely determined by precipitation rather than glacial melt dynamics.

# 5.2 | Comparisons with other proglacial catchments

The sediment yield for the Mingyong Glacier catchment is relatively high compared with sediment yields from other glacierized basins on the Tibetan Plateau (Figure 8). On the Tibetan Plateau, sediment yields from glacierized basins generally decrease with increasing basin area (Figure 8a), and increase with greater glacier coverage (Figure 8b), which is in line with observations at a global scale (Milliman & Farnsworth, 2011). The high sediment yield of the Mingyong glacial catchment can be explained by its small but heavily glacierized (68%) basin area and the short distance between the sampling station and glacier snout (Hallet et al., 1996; Wulf et al., 2012). The

observed inverse relationship between sediment load and basin area might be because larger basins have poorer sediment delivery ratio due to increased sediment storage and weakened sediment connectivity (Walling, 1983; Wohl et al., 2019).

The high variation of annual suspended sediment yield might be induced by what is known as threshold effect in sediment transport, with disproportionally high sediment delivery efficacy in excess of the critical level (Lane & Nienow, 2019). In addition, the type of substrate and subglacial deposits, rates of glacier movement, characteristics of the glacier drainage system, and the basin topography can affect the interannual variability of sediment yields (Herman et al., 2021). The competing effects of these confounding factors could be further investigated in a future study.

Furthermore, small glacierized basins generate disproportionally high sediment yield because a high transport efficacy can be sustained by short sediment transport distance, steep valley gradients, and high stream power of glacier melt flow (Gurnell et al., 1996; Wulf et al., 2012). In the Mingyong Glacier catchment, the sampling station is 3 km downstream from the glacier snout and the slope ranges from 9% to 71% (Figure S1a). Apart from its physical setting, the relatively high precipitation in the Mingyong catchment (over 600 mm/year) also contributes to its high sediment mobilization and yield (Table 2). For example, the summer rainfall can flush the supraglacial debris cover and proglacial sediment storage in large volumes downstream (Riihimaki, 2005; Srivastava et al., 2014). Increased snowmelt and rainfall during the onset of the thaw season can also increase water infiltration from the surface of the glacier to the base and enhance the subglacial drainage system, thereby facilitating the export of subglacial sediment (Alley et al., 1997; Delaney & Adhikari, 2020).

### 5.3 | Implications for the Lower Mekong River

Our quantification of sediment fluxes from the Mingyong Glacier catchment provides baseline measurements to better understand changes in erosion rates within the context of wider climatic

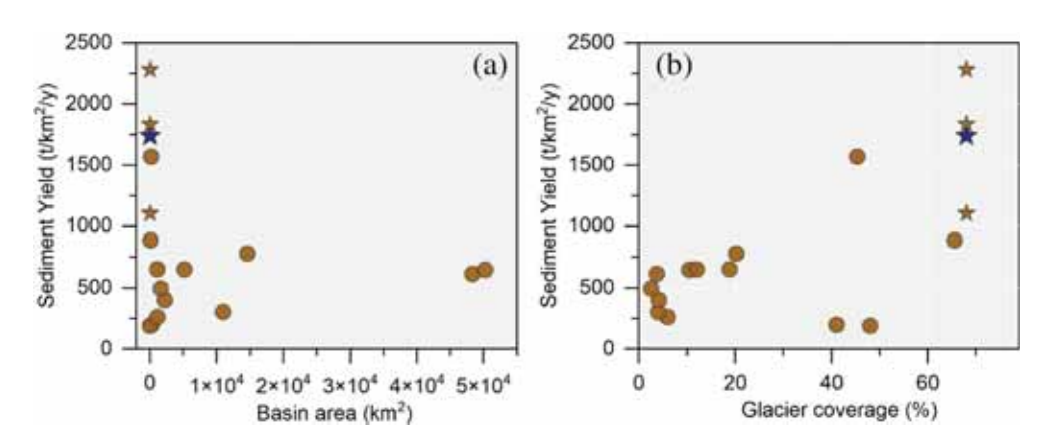


**FIGURE 8** Sediment yields versus (a) basin areas and (b) glacier coverage percent. The sediment yields of brown dots were collected from previous publications. Brown stars represent the sediment yields observed during three individual hydrological years and the blue stars represent the average sediment yield during three hydrological years in the Mingyong catchment during this study

TABLE 2 Locations and hydroclimatic characteristics of sediment yield observations from glacierized basins on the Tibetan Plateau and surrounding mountains

					1					
Basin	Observation period	Lat. (°N)	Lon. (°E)	Temperature (°C)	Precipitation (mm)	Basin area (km²)	Glacier coverage (%)	Water discharge (km³/year)	Sediment yield (t/km²/year)	Source
Mingyong	2013	28.47	98.78	9.9	526	39.7	89	0.5	1104	This study
Mingyong	2015	28.47	98.78	6.4	722	39.7	89	0.5	2281	
Mingyong	2016	28.47	98.78	6.7	029	39.7	89	0.46	1833	
Keqikar River	2018	41.81	80.17	9.0	456	110	65.5	0.53	890	Zhao et al. (2021)
Rongbu River	2018	27.98	86.92	3.9	266	280	41	0.075	200	
Kalasu River	1960-2004	42	82	7.4	125	1114	5.92	0.0024	263	
Pishan River	1960-2016	37.22	78.77	7.0	174	2227	4.1	0.959	403	
Santun River	1960-2016	43.72	86.92	7.8	278	1636	2.5	0.0445	496	
Manas River	1959-2007	44	85.77	0.9	200	5156	12	6.517	653	
Bayingou River	1983-2008	44.02	84.98	4.5	291	1092	18.8	4.422	654	
Yulongkashi River	1960-2010	37	79.03	-7.5	323	14 575	20.2	0.331	782	
Yerkang River	1960-2017	37.98	76.9	-4.7	234	50 200	10.5		920	Li, Lu, et al. (2021); Li,
Shule River	1960-2016	39.82	96.25	5.0	54	10 961	4	0.233	304	Overeem, et al. (2021)
Urumqi glacier No. 1 catchment	2004-2008	43.1	86.82	-5.9	504	3.34	48	0.206	191	Li et al. (2012)
Sutlej River	2001-2009	39.82	78	1	1	48 316	3.7	0.354	615	Wulf et al. (2012)
Hailuogon basin	2008, 2013	29.57	101.98	4.6	1881	178	45.3	2.254	1570	Li et al. (2019)

 ${\it Note:} \ {\it See Carrivick and Tweed (2021) for sediment yields from regions outside of the Tibetan Plateau.}$ 

LU ET AL. WILEY 11 of 13

alterations (Li, Lu, et al., 2021; Li, Overeem, et al., 2021). Because the Mingyong Glacier region is in the upper reaches of the Mekong and Salween Rivers, our study also provides insights into the contribution of sediment to the upper reaches of these transboundary rivers under the fast pace of temperature increase (Figure 2c). For the Mekong Glacier catchment, a better understanding of sediment supply and delivery in its entire basin is needed for better management of its sediment fluxes, as one major issue is the potential impacts of sediment loads on Chinese dams in the Mekong River. Before Manwan Dam was constructed in 1992, the upper Mekong reach in China provided around 80 million tons of sediment to the lower Mekong reach (Lu et al., 2014; Lu & Siew, 2006; Wang et al., 2011). However, the high sediment supply from the proglacial catchments in the headwater region cannot be transported downstream because of the series of cascade dams constructed in the Upper Mekong River. The sediment load below these cascade dams in Yunnan has dropped to around 10% of the pre-dam level (Chua & Lu, 2022a, 2022b; Sun et al., 2022). Subsequently, the problem of sediment starvation due to the trapping of sediment by reservoirs will get worse in the future with more dams being planned or built. Further down the Mekong Basin, the declining sediment flux combined with regional sand-mining and water withdrawal for crop irrigation, has contributed to drastic water level reductions in the Cambodian floodplains and Vietnamese delta (Chua et al., 2022; Chua & Lu, 2022a, 2022b; Lu & Chua, 2021).

### 6 | CONCLUSIONS

The Mingyong Glacier catchment in the upper Mekong basin is characterized by distinct wet and dry seasons, with discharge and suspended sediment concentrations increasing from February to July and decreasing from August to January. The yearly variations in sediment load for the Mingyong Glacier are large (44 kt in 2013, 91 kt in 2015, and 73 kt in 2016), despite small variations in water discharge. More than 65% of the annual sediment load is contributed between June and August. These observed seasonal variations in the sediment load indicate the complex competing influences of the supply and storage of suspended sediment load. Specifically, the clockwise hysteresis relationship suggests that sediment is stored during the low flow season and transported when flow increases from February to July, with the exhaustion of sediment supply after July. Even though discharge and SSC are generally positively correlated, seasonal variations result in different sediment rating relationships due to the influence of glacial meltwater. Based on the in-situ observations over three hydrological years, the sediment yields are estimated to be 1104 t/km<sup>2</sup>/year in 2013, 2283 t/km<sup>2</sup>/year in 2015, and 1833 t/km<sup>2</sup>/year in 2016.

This study provides baseline measurements for potential future monitoring of the glacial catchment in response to climate change. Concurrently, the data fills the knowledge gap in sediment data for the headwaters of the Mekong River. As this study was conducted insitu, the hand collection of water samples for filtration, hand implementation of the float chamber method, and hand measurements of water depth could introduce random errors. Thus, the use of specific automated hydrology equipment in subsequent studies such as data

loggers or turbidity meters could increase the sampling frequency and accuracy of future sediment load estimates. Furthermore, installation of a nearby weather monitoring station would give more insight into the diurnal and seasonal ablation patterns of the Mingyong Glacier, allowing better attribution of the variation in its discharge or transport capacity to climatic or other environmental factors.

### **ACKNOWLEDGEMENT**

The first author, Xixi Lu, would like to express his sincere thanks to Professor Des Walling for his support, encouragement and inspiration over many years. This study was supported by the National University of Singapore (A-0003626-00-00) and the Yunnan University of Finance and Economics. The work was also supported by the studentship awarded to Boey Lai Hsia from the Yunnan University of Finance and Economics. We want to thank Professor Zhou Yue, Yunnan University of Finance and Economics, for his support to our work in Yunnan. We also want to thank Professor Bruce Webb for his invitation and editing the special issue.

#### **DATA AVAILABILITY STATEMENT**

The water discharge and sediment concentration data can be obtained from the correspoding authors upon request.

#### **ORCID**

Xixi Lu https://orcid.org/0000-0002-2528-4631

Ting Zhang https://orcid.org/0000-0003-4975-0200

Dongfeng Li https://orcid.org/0000-0003-0119-5797

#### **REFERENCES**

Alley, R. B., Cuffey, K. M., Evenson, E. B., Strasser, J. C., Lawson, D. E., & Larson, G. J. (1997). How glaciers entrain and transport basal sediment: Physical constraints. *Quaternary Science Reviews*, 16(9), 1017–1038. https://doi.org/10.1016/S0277-3791(97)00034-6

Asselman, N. E. M. (2000). Fitting and interpretation of sediment rating curves. *Journal of Hydrology*, 234(3), 228–248. https://doi.org/10.1016/S0022-1694(00)00253-5

Baker, B. B., & Moseley, R. K. (2007). Advancing treeline and retreating glaciers: Implications for conservation in Yunnan, P.R. China. Arctic, Antarctic, and Alpine Research, 39(2), 200–209. https://doi.org/10. 1657/1523-0430(2007)39[200:Atargi]2.0.Co;2

Beck, H. E., Zimmermann, N. E., McVicar, T. R., Vergopolan, N., Berg, A., & Wood, E. F. (2018). Present and future Koppen-Geiger climate classification maps at 1-km resolution. *Scientific Data*, 5, 180214. https://doi.org/10.1038/sdata.2018.214

Bennett, M. M., & Glasser, N. F. (2011). Glacial geology: Ice sheets and landforms. John Wiley & Sons.

Beylich, A. A., Laute, K., & Storms, J. E. A. (2017). Contemporary suspended sediment dynamics within two partly glacierized mountain drainage basins in western Norway (Erdalen and Bødalen, inner Nordfjord). Geomorphology, 287, 126–143. https://doi.org/10.1016/j.geomorph.2015.12.013

Carrillo, R., & Mao, L. (2020). Coupling sediment transport dynamics with sediment and discharge sources in a glacial Andean basin. *Water*, 12(12), 3452. https://doi.org/10.3390/w12123452

Carrivick, J. L., & Tweed, F. S. (2021). Deglaciation controls on sediment yield: Towards capturing spatio-temporal variability. *Earth-Science Reviews*, 221, 103809. https://doi.org/10.1016/j.earscirev.2021.103809

Chakrapani, G. J., & Saini, R. K. (2009). Temporal and spatial variations in water discharge and sediment load in the Alaknanda and Bhagirathi



- Rivers in Himalaya, India. Journal of Asian Earth Sciences, 35(6), 545–553. https://doi.org/10.1016/j.jseaes.2009.04.002
- Chua, S. D. X., & Lu, X. X. (2022a). What can stage curves tell us about water level changes? Case study of the lower Mekong Basin. *Catena*, 216. 106385.
- Chua, S. D. X., & Lu, X. X. (2022b). Sediment load crisis in the Mekong River basin: Severe reductions over the decades. Available at SSRN 4167753.
- Chua, S. D. X., Lu, X. X., Oeurng, C., Sok, T., & Grundy-Warr, C. (2022). Drastic decline of flood pulse in the Cambodian floodplains (Mekong River and Tonle Sap system). *Hydrology and Earth System Sciences*, 26(3), 609–625.
- Costa, A., Molnar, P., Stutenbecker, L., Bakker, M., Silva, T. A., Schlunegger, F., Lane, S., Loizeau, J.-L., & Girardclos, S. (2018). Temperature signal in suspended sediment export from an alpine catchment. *Hydrology and Earth System Sciences*, 22(1), 509–528. https:// doi.org/10.5194/hess-22-509-2018
- Delaney, I., & Adhikari, S. (2020). Increased subglacial sediment discharge in a warming climate: Consideration of ice dynamics, glacial erosion, and fluvial sediment transport. *Geophysical Research Letters*, 47(7), e2019GL085672. https://doi.org/10.1029/2019gl085672
- Delaney, I., Bauder, A., Werder, M. A., & Farinotti, D. (2018). Regional and annual variability in subglacial sediment transport by water for two glaciers in the Swiss Alps. Frontiers in Earth Science, 6, 175. https://doi. org/10.3389/feart.2018.00175
- Eyles, N. (2006). The role of meltwater in glacial processes. *Sedimentary Geology*, 190(1–4), 257–268. https://doi.org/10.1016/j.sedgeo.2006. 05.018
- Gatesman, T. A. (2017). Glacier contribution to lowland streamflow: A multiyear, geochemical hydrograph separation study in sub-Arctic. University of Alaska Fairbanks.
- Gurnell, A., Hannah, D., & Lawler, D. (1996). Suspended sediment yield from glacier basins. IAHS Publications-Series of Proceedings and Reports-Intern Assoc Hydrological Sciences, 236, 97–104.
- Hallet, B., Hunter, L., & Bogen, J. (1996). Rates of erosion and sediment evacuation by glaciers: A review of field data and their implications. *Global and Planetary Change*, 12(1), 213–235. https://doi.org/10. 1016/0921-8181(95)00021-6
- He, Y. Q., Zhang, Z. L., Theakstone, W. H., Chen, T., Yao, T. D., & Pang, H. X. (2003). Changing 637 features of the climate and glaciers in China's monsoonal temperate glacier region. *Journal of Geophysical Research*: Atmospheres, 108, 1–7. https://doi.org/10.1029/2002JD003365
- Heckmann, T., McColl, S., & Morche, D. (2016). Retreating ice: Research in pro-glacial areas matters. Earth Surface Processes and Landforms, 41(2), 271–276. https://doi.org/10.1002/esp.3858
- Herman, F., De Doncker, F., Delaney, I., Prasicek, G., & Koppes, M. (2021). The impact of glaciers on mountain erosion. *Nature Reviews Earth & Environment*, 2(6), 422–435. https://doi.org/10.1038/s43017-021-00165-9
- Khanchoul, K., & Jansson, M. B. (2008). Sediment rating curves developed on stage and seasonal means in discharge classes for the Mellah Wadi, Algeria. Geografiska Annaler. Series A, Physical Geography, 90(3), 227–236.
- Kirschbaum, D., Kapnick, S. B., Stanley, T., & Pascale, S. (2020). Changes in extreme precipitation and landslides over High Mountain Asia. Geophysical Research Letters, 47(4), e2019GL085347. https://doi.org/10. 1029/2019gl085347
- Kumar, K., Miral, M. S., Joshi, V., & Panda, Y. S. (2002). Discharge and suspended sediment in the meltwater of Gangotri Glacier, Garhwal Himalaya, India. *Hydrological Sciences Journal*, 47(4), 611–619. https://doi.org/10.1080/02626660209492963
- Lane, S. N., & Nienow, P. W. (2019). Decadal-scale climate forcing of alpine glacial hydrological systems. Water Resources Research, 55(3), 2478–2492. https://doi.org/10.1029/2018wr024206

- Lau, W. K. M., Kim, M.-K., Kim, K.-M., & Lee, W.-S. (2010). Enhanced surface warming and accelerated snow melt in the Himalayas and Tibetan Plateau induced by absorbing aerosols. *Environmental Research Letters*, 5(2), 025204. https://doi.org/10.1088/1748-9326/5/2/025204
- Li, D., Li, Z., Zhou, Y., & Lu, X. (2020). Substantial increases in the water and sediment fluxes in the headwater region of the Tibetan Plateau in response to global warming. *Geophysical Research Letters*, 47(11), e2020GL087745. https://doi.org/10.1029/2020GL087745
- Li, D., Lu, X., Overeem, I., Walling, D. E., Syvitski, J., Kettner, A. J., Bookhagen, B., Zhou, Y., & Zhang, T. (2021). Exceptional increases in fluvial sediment fluxes in a warmer and wetter High Mountain Asia. Science, 374(6567), 599–603. https://doi.org/10.1126/science.abi9649
- Li, D., Overeem, I., Kettner, A. J., Zhou, Y., & Lu, X. (2021). Air temperature regulates erodible landscape, water, and sediment fluxes in the permafrost-dominated catchment on the Tibetan Plateau. Water Resources Research, 57(2), e2020WR028193. https://doi.org/10. 1029/2020WR028193
- Li, X., Ding, Y., Liu, Q., Zhang, Y., Han, T., Jing, Z., Yu, Z., Li, Q., & Liu, S. (2019). Intense chemical weathering at glacial meltwater-dominated Hailuogou Basin in the southeastern Tibetan Plateau. *Water*, 11(6), 1209. https://doi.org/10.3390/w11061209
- Li, Z., Gao, W., Zhang, M., & Gao, W. (2012). Variations in suspended and dissolved matter fluxes from glacial and non-glacial catchments during a melt season at Urumqi River, eastern Tianshan, Central Asia. *Catena*, 95, 42–49. https://doi.org/10.1016/j.catena.2012.03.002
- Liu, Q., Liu, S. Y., Guo, W. Q., Yong, N., Donghui, S. G., Xu, J. L., & Yao, X. J. (2015). Glacier changes in the Lancang River Basin, China, between 1968-1975 and 2005-2010. Arctic, Antarctic, and Alpine Research, 47, 335-344. https://doi.org/10.1657/AAAR0013-104
- Lloyd, C. E. M., Freer, J. E., Johnes, P. J., & Collins, A. L. (2016). Using hysteresis analysis of high-resolution water quality monitoring data, including uncertainty, to infer controls on nutrient and sediment transfer in catchments. Science of the Total Environment, 543(Pt A), 388–404. https://doi.org/10.1016/j.scitotenv.2015.11.028
- Lu, X. X., & Chua, S. D. X. (2021). River discharge and water level changes in the Mekong River: Droughts in an era of mega-dams. *Hydrological Processes*, 35(7), e14265.
- Lu, X. X., Kummu, M., & Oeurng, C. (2014). Reappraisal of sediment dynamics in the Lower Mekong River, Cambodia. Earth Surface Processess & Landfomrs, 39(14), 1855–1865. https://doi.org/10.1002/esp. 3573
- Lu, X. X., & Siew, R. Y. (2006). Water discharge and sediment flux changes over the past decades in the Lower Mekong River: Possible impacts of the Chinese dams. Hydrology and Earth System Sciences, 10(2), 181–195.
- Lugon, R., & Stoffel, M. (2010). Rock-glacier dynamics and magnitude-frequency relations of debris flows in a high-elevation watershed: Ritigraben, Swiss Alps. Global and Planetary Change, 73(3-4), 202-210. https://doi.org/10.1016/j.gloplacha.2010.06.004
- Mao, L., & Carrillo, R. (2017). Temporal dynamics of suspended sediment transport in a glacierized Andean basin. *Geomorphology*, 287, 116– 125. https://doi.org/10.1016/j.geomorph.2016.02.003
- Mao, L., Comiti, F., Carrillo, R., & Penna, D. (2019). Sediment transport in proglacial rivers. In T. Heckmann & D. Morche (Eds.), Geomorphology of proglacial systems: Landform and sediment dynamics in recently deglaciated alpine landscapes (pp. 199–217). Springer International Publishing.
- Micheletti, N., & Lane, S. N. (2016). Water yield and sediment export in small, partially glaciated alpine watersheds in a warming climate. *Water Resources Research*, 52(6), 4924–4943. https://doi.org/10.1002/2016wr018774
- Miles, K. E., Hubbard, B., Irvine-Fynn, T. D. L., Miles, E. S., Quincey, D. J., & Rowan, A. V. (2020). Hydrology of debris-covered glaciers in High Mountain Asia. *Earth-Science Reviews*, 207, 103212. https://doi.org/ 10.1016/j.earscirev.2020.103212

- Milliman, J. D., & Farnsworth, K. L. (2011). Runoff, erosion, and delivery to the coastal ocean. In J. D. Milliman & K. L. Farnsworth (Eds.), *River discharge to the coastal ocean*: A *global synthesis* (pp. 13–69). Cambridge University Press.
- Overeem, I., Hudson, B. D., Syvitski, J. P. M., Mikkelsen, A. B., Hasholt, B., van den Broeke, M. R., Noël, B. P. Y., & Morlighem, M. (2017). Substantial export of suspended sediment to the global oceans from glacial erosion in Greenland. *Nature Geoscience*, 10(11), 859–863. https://doi.org/10.1038/ngeo3046
- Pepin, N., Bradley, R. S., Diaz, H. F., Baraer, M., Caceres, E. B., Forsythe, N., Fowler, H., Greenwood, G., Hashmi, M., Liu, X., Miller, J., Ning, L., Ohmura, A., Palazzi, E., Rangwala, I., Schöner, W., Severskiy, I., Shahgedanova, M., Wang, M., & Yang, D. (2015). Elevation-dependent warming in mountain regions of the world. *Nature Climate Change*, 5(5), 424–430. https://doi.org/10.1038/nclimate2563
- Riihimaki, C. A., MacGregor, K. R., Anderson, R. S., Anderson, S. P., & Loso, M. G. (2005). Sediment evacuation and glacial erosion rates at a small alpine glacier. *Journal of Geophysical Research: Earth Surface*, 110(F3). https://doi.org/10.1029/2004jf000189
- Rosser, N. J. (2010). Landslides and rockfalls. In *Sediment cascades: An Integrated Approach* (pp. 55–87). Wiley Online Library.
- Shi, X., Zhang, F., Lu, X., Wang, Z., Gong, T., Wang, G., & Zhang, H. (2018). Spatiotemporal variations of suspended sediment transport in the upstream and midstream of the Yarlung Tsangpo River (the upper Brahmaputra), China. Earth Surface Processes and Landforms, 43(2), 432–443. https://doi.org/10.1002/esp.4258
- Singh, A. T., Sharma, P., Sharma, C., Laluraj, C. M., Patel, L., Pratap, B., Oulkar, S., & Thamban, M. (2020). Water discharge and suspended sediment dynamics in the Chandra River, Western Himalaya. *Journal of Earth System Science*, 129(1), 1–15. https://doi.org/10.1007/s12040-020-01455-4
- Smith, H. G., & Dragovich, D. (2009). Interpreting sediment delivery processes using suspended sediment-discharge hysteresis patterns from nested upland catchments, South-Eastern Australia. *Hydrological Processes*, 23(17), 2415–2426. https://doi.org/10.1002/hyp.7357
- Srivastava, D., Kumar, A., Verma, A., & Swaroop, S. (2014). Characterization of suspended sediment in meltwater from glaciers of Garhwal Himalaya. *Hydrological Processes*, 28(3), 969–979. https://doi.org/10.1002/hyp.9631
- Stott, T., & Mount, N. (2007). Alpine proglacial suspended sediment dynamics in warm and cool ablation seasons: Implications for global warming. *Journal of Hydrology*, 332(3–4), 259–270. https://doi.org/10. 1016/j.jhydrol.2006.07.001
- Sun, L., Sun, Z., Li, Z., Zheng, H., Li, C., & Xiong, W. (2022). Response of runoff and suspended load to climate change and reservoir construction in the Lancang River. *Journal of Water and Climate Change*, 13(4), 1966–1984.
- Walling, D. E. (1983). The sediment delivery problem. *Journal of Hydrology*, 65(1), 209–237. https://doi.org/10.1016/0022-1694(83)90217-2
- Walling, D. E. (2006). Human impact on land-ocean sediment transfer by the world's rivers. *Geomorphology*, 79(3-4), 192-216. https://doi.org/10.1016/j.geomorph.2006.06.019

- Walling, D. E. (2008). The changing sediment load of the Mekong River. Ambio, 37, 150-157.
- Wang, J. J., Lu, X. X., & Kummu, M. (2011). Sediment load estimates and variations in the Lower Mekong River. River Research and Applications, 27(1), 33–46.
- Williams, G. P. (1989). Sediment concentration versus water discharge during single hydrologic events in rivers. *Journal of Hydrology*, 111(1), 89–106. https://doi.org/10.1016/0022-1694(89)90254-0
- Wohl, E., Brierley, G., Cadol, D., Coulthard, T. J., Covino, T., Fryirs, K. A., Grant, G., Hilton, R., Lane, S., Magilligan, F., Meitzen, K., Passalacqua, P., Pöppl, R., Rathburn, S., & Sklar, L. S. (2019). Connectivity as an emergent property of geomorphic systems. *Earth Surface Processes and Landforms*, 44(1), 4–26. https://doi.org/10.1002/esp.4434
- Wulf, H., Bookhagen, B., & Scherler, D. (2010). Seasonal precipitation gradients and their impact on fluvial sediment flux in the northwest Himalaya. *Geomorphology*, 118(1-2), 13-21. https://doi.org/10.1016/j.geomorph.2009.12.003
- Wulf, H., Bookhagen, B., & Scherler, D. (2012). Climatic and geologic controls on suspended sediment flux in the Sutlej River Valley, Western Himalaya. Hydrology and Earth System Sciences, 16(7), 2193–2217. https://doi.org/10.5194/hess-16-2193-2012
- Yaksich, S. M., & Verhoff, F. H. (1983). Sampling strategy for river pollutant transport. *Journal of Environmental Engineering*, 109(1), 219–231. https://doi.org/10.1061/(ASCE)0733-9372(1983)109:1(219)
- Yao, T., Thompson, L., Yang, W., Yu, W., Gao, Y., Guo, X., Yang, X., Duan, K., Zhao, H., Xu, B., Pu, J., Lu, A., Xiang, Y., Kattel, D., & Joswiak, D. (2012). Different glacier status with atmospheric circulations in Tibetan Plateau and surroundings. *Nature Climate Change*, 2(9), 663–667. https://doi.org/10.1038/nclimate1580
- Zhang, T., Li, D., Kettner, A. J., Zhou, Y., & Lu, X. (2021). Constraining dynamic sediment-discharge relationships in cold environments: The sediment-availability-transport (SAT) model. Water Resources Research, 57(10), e2021WR030690. https://doi.org/10.1029/2021wr030690
- Zhao, Y., Ma, W., Han, H., Zhuang, S., Shi, H., Ding, Y., & Lu, X. (2021). Suspended sediment transport characteristics of glacial rivers in alpine mountainous areas. *Bulletin of Soil and Water Conservation*, 41(3), 94–102 (in Chinese).

#### SUPPORTING INFORMATION

Additional supporting information can be found online in the Supporting Information section at the end of this article.

How to cite this article: Lu, X., Zhang, T., Hsia, B. L., Li, D., Fair, H., Niu, H., Chua, S. D. X., Li, L., & Li, S. (2022). Proglacial river sediment fluxes in the southeastern Tibetan Plateau: Mingyong Glacier in the Upper Mekong River. *Hydrological Processes*, *36*(11), e14751. <a href="https://doi.org/10.1002/hyp.14751">https://doi.org/10.1002/hyp.14751</a>